PNAS RESEARCH ARTICLE | ECOLOGY

Multikingdom interactions govern the microbiome in subterranean cultural heritage sites

Wenjing Liu[a,b], Xiaoai Zhou[c], Tao Jin[d], Yonghui Li[e,f], Bin Wu[g], Daoyuan Yu[h], Zongren Yu[i], Bomin Su[i,1], Ruirui Chen[a], Youzhi Feng[a,1], and Manuel Delgado-Baquerizo[j,k]

Edited by Dianne Newman, California Institute of Technology, Pasadena, CA; received December 2, 2021; accepted February 16, 2022

Microbial biodeterioration is a major concern for the conservation of historical cultural relics worldwide. However, the ecology involving the origin, composition, and establishment of microbiomes on relics, once exposed to external environments, is largely unknown. Here, we combined field surveys with physiological assays and biological interaction experiments to investigate the microbiome in the Dahuting Han Dynasty Tomb, a Chinese tomb with more than 1,800 y of history, and its surrounding environments. Our investigation finds that multikingdom interactions, from mutualism to competition, drive the microbiome in this subterranean tomb. We reveal that Actinobacteria, Pseudonocardiaceae are the dominant organisms on walls in this tomb. These bacteria produce volatile geosmin that attracts springtails (Collembola), forming an interkingdom mutualism, which contributes to their dispersal, as one of the possible sources into the tomb from surrounding environments. Then, intrakingdom competition helps explain why Pseudonocardiaceae thrive in this tomb via the production of a mixture of cellulases, in combination with potential antimicrobial substances. Together, our findings show that multikingdom interactions play an important role in governing the microbiomes that colonize cultural relics. This knowledge is integral to understanding the ecological and physiological features of relic microbiomes and to supporting the relics' long-term conservation.

mutualism | antagonism | Actinobacteria | arthropods | geosmin

Significance

The conservation of historical relics against microbial biodeterioration is critical to preserving cultural heritages. One major challenge is our limited understanding of microorganisms' dispersal, colonization, and persistence on relics after excavation and opening to external environments. Here, we investigate the ecological and physiological profiles of the microbiome within and outside the Dahuting Han Dynasty Tomb with a 1,800-y history. Actinobacteria dominate the microbiome in this tomb. Via interkingdom signaling mutualism, springtails carry Actinobacteria as one possible source into the tomb from surrounding environments. Subsequently, Actinobacteria produce cellulases combined with antimicrobial substances, which helps them to colonize and thrive in the tomb via intrakingdom competition. Our findings unravel the ecology of the microbiomes colonizing historical relics and provide help for conservation practices.

Historical cultural relics are symbols of ancient cultures and arts and need to be protected for future generations. However, ancient relics are very vulnerable to biological activity (e.g., biodeterioration) in interaction with physical and/or chemical aggressions, especially when open to external environments (1–3). Complex and diverse microbial communities can colonize these relics and, in many cases, they contribute to the deterioration of these items (4–6). Microorganisms that thrive on relics might be just a reflection of the surrounding environmental microbiome (7). Yet, little is known about the ecology involving the origin, composition, and establishment of microbiomes on cultural relics (3, 8). This knowledge is the first step toward the development of high-throughput strategies to ensure the long-term conservation of cultural relics.

The microbiomes colonizing cultural relics in ancient tombs and/or caves are often dominated by a few supercompetitive microorganisms. For instance, Actinobacteria are often dominant in tombs and caves worldwide (5, 9–11) and can drive the biodeterioration of inside items via the production of organic acids, the formation of biofilms, the penetration of relic materials, and/or the excretion of a mixture of cellulolytic enzymes (12–14). However, the provenance of these microorganisms, their dispersion media, and how they outcompete others in tombs and/or caves remain poorly understood. Multiple theories could explain the mechanisms of microorganisms to disperse and thrive in these environments alone or in combination. First, interspecies mutualism can help the dispersal of microorganisms (15). Actinobacteria have been reported to release geosmin and 2-methylisoborneol, terpenoid substances which can attract soil-dwelling arthropods (e.g., springtails) as food sources and/or defensive symbionts (16) to help them disperse in fecal pellets and/or attach to bodies when arthropods move around (17). Such a dispersal mechanism could partly explain the dominance of Actinobacteria in ancient tombs and/or caves. Second, two types of intraspecies competition have been recognized in ecology, namely exploitative and interference competitions (18). The first form indicates that species indirectly compete through resource exploitation, while the second form indicates that one species directly harms another via, for example, antibiotic substances. Actinobacteria could exclude and outnumber other bacteria on relics via a stronger metabolic capability, especially for recalcitrant organic matter degradations (19) and secondary metabolite excretions [e.g., antibiotics

Author contributions: B.S. and Y.F. designed research; W.L., X.Z., T.J., Y.L., B.W., D.Y., Z.Y., B.S., R.C., and Y.F. performed research; W.L. and Y.F. contributed new reagents/analytic tools; W.L., X.Z., T.J., Y.L., B.W., D.Y., Y.F., and M.D.-B. analyzed data; and W.L., Y.F., and M.D.-B. wrote the paper.

The authors declare no competing interest.

This article is a PNAS Direct Submission.

[1]To whom correspondence may be addressed. Email: suboming@hotmail.com or yzfeng@issas.ac.cn.

This article contains supporting information online at http://www.pnas.org/lookup/suppl/doi:10.1073/pnas.2121141119/-/DCSupplemental.

Published March 28, 2022.

(20)]. Thus, we hypothesize that a combination of multikingdom mutualistic and competitive relationships is one of the major reasons for the dominance of a few groups of microorganisms on relics in ancient tombs and/or caves. Such insightful knowledge of the ecology of relic microbiomes is fundamental to eliminating the organisms that lead to biodeterioration.

Here, we investigate the microbiome of the Dahuting Han Dynasty Tomb in China. The Dahuting Han Dynasty Tomb is a subterranean tomb (Fig. 1 and *SI Appendix*, Fig. S1) with more than 1,800 y of history, and has been open to natural environments for over 60 y. Being one of the largest excavated tombs of the Han Dynasty (202 BC to AD 220), it provides a detailed record of all aspects of daily life (i.e., sacrifice, cooking, costumes, and entertainment) at that time (Fig. 1*A*). To avoid unintended human impacts such as those reported for Lascaux Cave (Dordogne, France) (7) and Altamira Cave (Cantabria, Spain) (21), this tomb was closed to visitors in the 1990s. Thus, it provides an excellent site to investigate the ecological and physiological features of microbiomes of historical relics in the absence of human activity which could trigger acute and/or strong environmental perturbations. White colonies, visible to the naked eye, have developed pervasively on the tomb walls (Fig. 1 *B*–*E*). Scanning electron microscopy is used to identify the typical filamentous morphology of Actinobacteria (Fig. 1*F*).

We use ecological theories, next-generation sequencing strategies (both amplicon and shotgun metagenomics), physiological profiling assays (for screened strains), and biological interaction experiments to investigate the origin, composition, and establishment of the microbiome colonizing this emblematic relic. Our study aims to 1) investigate the contribution of interkingdom signaling interactions (Actinobacteria–arthropods) in explaining the dispersal of Actinobacteria in the tomb, and 2) identify specific cellulolytic enzymatic and antimicrobial machineries that allow these bacteria to colonize and dominate the microbiome in these environments via exploitative and interference competitions within the kingdom. We posit that these ecological (i.e., species biointeractions and composition dynamics) and physiological (i.e., genes coding for enzymes and metabolic pathways in metagenomics as well as the produced geosmin, cellulases, and antimicrobial substances of screened Actinobacteria strains) findings can provide insights for the conservation of historical cultural relics and remains.

Our study provides evidence that the family Pseudonocardiaceae within the phylum Actinobacteria are the dominant organisms in the Dahuting Han Dynasty Tomb and that their success in colonizing, thriving, and ruling such environments can be explained by interkingdom mutualistic (bacteria–Collembola) and intrakingdom competitive (bacteria–bacteria) interactions. In particular, our survey and experiments show that Actinobacteria–arthropod signaling interactions via geosmin (i.e., interkingdom mutualism) can partly explain how Actinobacteria disperse into the tomb from surrounding environments. Our physiological assays, based on Pseudonocardiaceae strains screened from this tomb, and metagenomic data further indicate that Actinobacteria produce a powerful mixture of cellulases that confers a greater substrate metabolic capability in their colonization of these environments over other bacteria (namely, intrakingdom exploitative competition); the intraspecies antagonism could also contribute to the dominance of Actinobacteria in this tomb (namely, intrakingdom interference competition). Together, our work highlights that multikingdom biological interactions contribute to the origin, composition, and establishment of the microbiomes responsible for the biodeterioration of historical cultural relics.

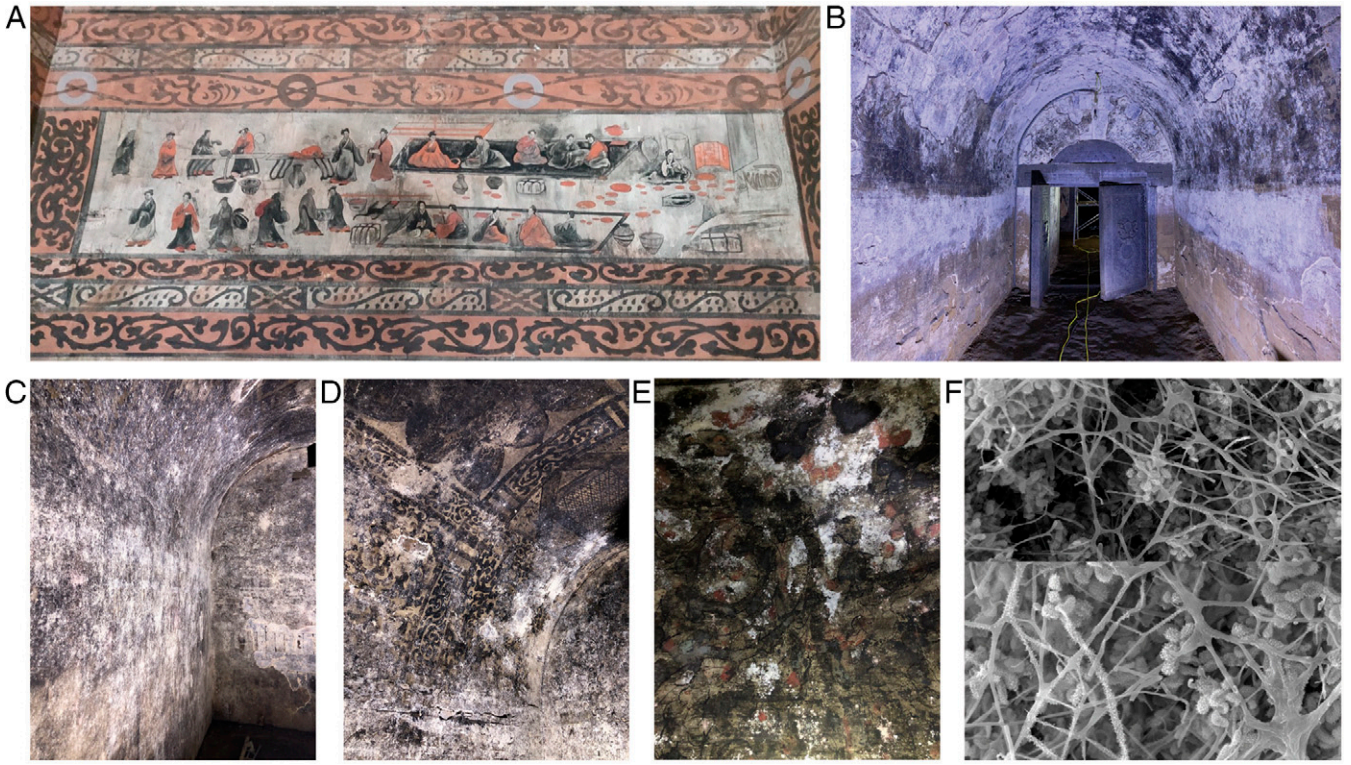

Fig. 1. Pictures of the Dahuting Han Dynasty Tomb, which has a 1,800-y history and has been open to environments for over 60 y. (*A*) The remarkable and sophisticated murals record the living and social activities of the people in the Han Dynasty (202 BC to AD 220). (*B*–*E*) White colonies, which are visible to the naked eye, are pervasive on tomb walls. (*F*) Photomicrographs of white colonies on walls presented by scanning electron microscopy.

Results and Discussion

Dominant Microbiome of the Tomb. Our results indicate that Actinobacteria taxa (in terms of operational taxonomic units; OTUs) are the dominant bacterial group in the Dahuting Han Dynasty Tomb, accounting for between 57.88 and 73.87% (an average of 67.17%) of all bacterial 16S ribosomal RNA (rRNA) reads among 10 tomb samples, based on amplicon sequencing, and between 32.77 and 41.71% (an average of 36.65%) of all bacterial reads, based on PCR bias–free shotgun metagenomic sequencing. Proteobacteria (21.28 and 24.37%), Acidobacteria (4.96 and 1.50%), and Planctomycetes (1.86 and 1.49%) (Fig. 2 and *SI Appendix*, Figs. S2*A* and S3*A*) are the next dominant bacteria in this tomb according to amplicon and metagenomic sequencing results. qPCR analyses confirm the dominance of bacteria vs. fungi and eukaryotes throughout the tomb (*SI Appendix*, Fig. S4). At higher resolution, family Pseudonocardiaceae taxa show the highest percentages within the phylum Actinobacteria, ranging from 73.26 to 95.01% (amplicon sequencing) and from 54.29 to 78.04% (shotgun metagenomics) (Fig. 2 and *SI Appendix*, Figs. S2*C* and S3*B*). We were further able to screen and culture eight strains affiliated with Pseudonocardiaceae from this tomb. Colony morphologies of these strains are exhibited in *SI Appendix*, Fig. S5. The white color of Pseudonocardiaceae strain colonies well aligns with those observed pervasively on the walls of the Dahuting Han Dynasty Tomb. Pseudonocardiaceae have been reported in subterranean tombs and caves worldwide, such as Doña Trinidad, Santimamiñe, and Altamira Cave in Spain (5, 9), Etruscan necropolises in Italy (10), and Lascaux Cave in France (11). Further amplicon sequencing analyses reveal that the most eukaryotic 18S rRNA reads belong to the phylum Arthropods (90.47%), order Collembola (71.59%) (Fig. 2 and *SI Appendix*, Fig. S2 *B* and *D*). It is consistent with the metagenomic result, with the highest (32.79%) eukaryotic reads belonging to arthropods (*SI Appendix*, Fig. S3*C*). The dominance of Collembola has also been observed in subterranean tombs and caves worldwide (11, 22–24).

Environmental Filtering Selects the Microbiome of the Tomb from Surrounding Soils. Both bacterial and eukaryotic community compositions substantially differ between the tomb and the surrounding soils, as indicated by a Jaccard distance-based redundancy analysis (RDA) (*SI Appendix*, Fig. S6 *A* and *B*) and a Bray–Curtis distance-based heatmap ($P < 0.01$) (*SI Appendix*, Fig. S6 *C* and *D*). Moreover, 94.69% of bacterial and 84.76% of eukaryotic taxa detected in the tomb are just subsets of those found in surrounding soils (Fig. 2). All the above information suggests that surrounding environments might provide species pools for the tomb (10, 11, 25) and herein some species are then selected via environmental filtering (26, 27). Subterranean tombs present relatively constant conditions, which is in contrast with the conditions in surrounding environments (*SI Appendix*, Fig. S7), and this stability might act as an environmental filter and explain these community differences. In fact, RDAs indicate that temperature and humidity stabilities, as well as the presence/absence of illumination, can help explain the differences in microbial community composition between environments inside and outside the tomb (*SI Appendix*, Fig. S6 *A* and *B*).

Multikingdom Ecological Network Thrives in the Tomb. Our analyses further reveal multiple associations between species within Actinobacteria and Collembola, as well as between Actinobacteria and other bacterial species. We constructed a cooccurrence network between Pseudonocardiaceae and Collembola taxa as well as other bacterial taxa (Fig. 3*A*) (*Materials and Methods*). The seven highest-abundance Collembola taxa show significantly positive correlations with the dominant Pseudonocardiaceae taxa (especially OTU1) (*SI Appendix*, Fig. S8*A*). In particular, the read abundance of Pseudonocardiaceae-like OTU1 accounts for more than 50% of the 101 Pseudonocardiaceae taxa in each sample. In contrast, significantly negative correlations between Pseudonocardiaceae-like OTU1 and 60 bacterial taxa are observed (*SI Appendix*, Fig. S8*B*). These bacterial taxa are mainly affiliated with a wide variety of phyla, such as Proteobacteria, Planctomycetes, Actinobacteria, Chloroflexi, Acidobacteria, Armatimonadetes, Gemmatimonadetes, Rokubacteria, Verrucomicrobia, and Bacteroidetes. This cooccurrence ecological network provides a benchmark for cause–effect investigations on inter- and intrakingdom interactions that can explain the Actinobacteria, Pseudonocardiaceae-dominant microbiome in the tomb.

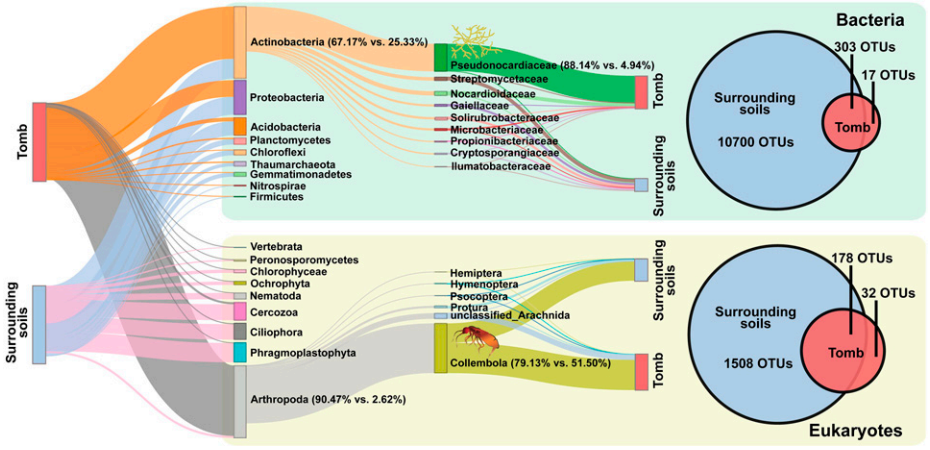

Fig. 2. Amplicon reads indicate that the phyla Actinobacteria and Arthropoda taxa (in terms of reads) dominate bacterial and eukaryotic communities in the tomb, which are up to 67.17 and 90.47%, respectively. At higher resolution, the family Pseudonocardiaceae and order Collembola exhibit the highest percentages of the phylum Actinobacteria and all Arthropoda taxa, accounting for 88.14 and 79.13%, respectively. Venn analyses indicate the shared and specific bacterial and eukaryotic taxa within and between the Dahuting Han Dynasty Tomb and surrounding soils. Herein, 94.69% of bacterial and 84.76% of eukaryotic taxa in the tomb are detected in surrounding soils, indicating that the species in the tomb are just subsets of those in surrounding environments.

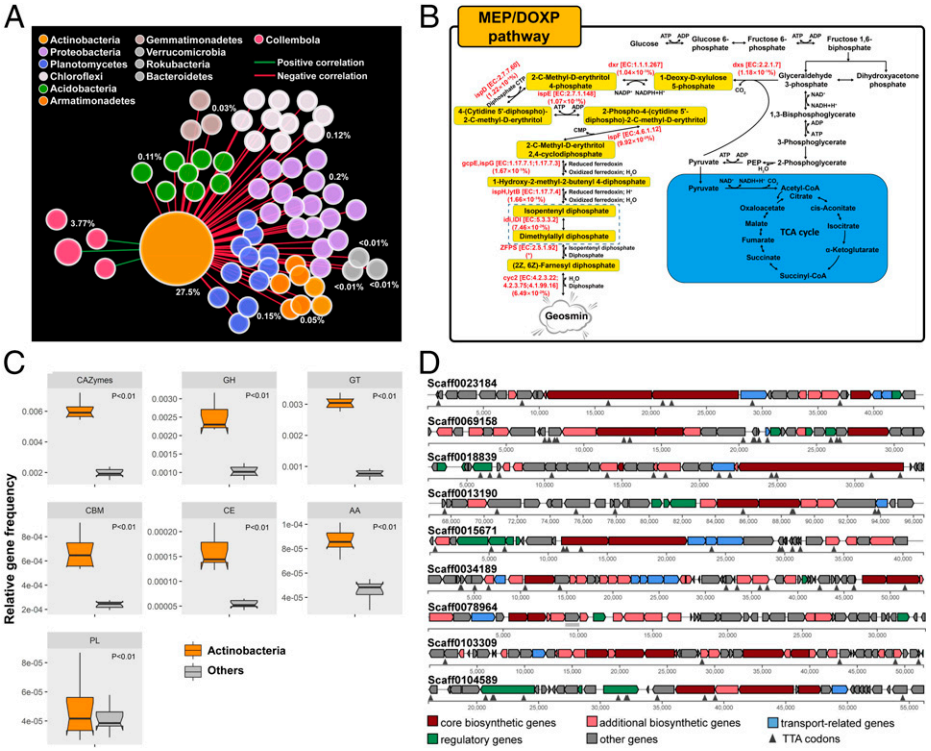

Fig. 3. Ecological cooccurrence network of the significant interactions between Pseudonocardiaceae and Collembola taxa as well as other bacterial taxa (*A*). Positively and negatively interacting taxa are connected by green and red lines, respectively. The size of the circle is proportional to the average relative abundances in total bacterial or eukaryotic reads derived from amplicon sequencing, numbered near the circle. The integrated geosmin biosynthesis pathway in the pivotal Actinobacteria bin (*B*). The metabolic pathway and associated key enzymes as well as relative gene frequencies are detected in the whole-gene sequences of the pivotal bin (regarding the functions of Actinobacteria) regenerated from shotgun metagenomics from 10 samples in the tomb. The percentage in the parentheses near the line is the relative frequency of the gene-encoding enzyme in the pivotal bin. Note: The asterisk indicates that the relative gene frequency is lower than the detection line. DOXP, 1-deoxy-D-xylulose 5-phosphate; MEP, 2-C-methyl-D-erythritol 4-phosphate; TCA, tricarboxylic acid. Comparison of the relative frequency of CAZymes encoding genes between Actinobacteria and other bacterial taxa detected in the shotgun metagenomics of 10 tomb samples (*C*). Gene clusters coding for the biosyntheses of several representative antimicrobial substances in the pivotal Actinobacteria bin (*D*). Herein, Scaff0023184 is the gene cluster coding for okaramine D and neopolyoxin C; Scaff0069158 is for thienamycin; Scaff0018839 is for showdomycin; Scaff0013190 is for okaramine D and neopolyoxin C; Scaff0015671 is for aurachin RE; Scaff0034189 is for xenematide; Scaff0078964 is for naphtocyclinone; Scaff0103309 is for strobilurin, curacomycin, and promysalin; and Scaff0104589 is for curacomycin, bicornutin A1, bicornutin A2, and okaramine D.

Interkingdom Mutualism Helps Actinobacteria Disperse into the Tomb from the Outside. Interkingdom signaling mutualism can explain how springtails help Actinobacteria disperse into the tomb. RDA indicates positive correlations between the relative abundances of Pseudonocardiaceae ($R = 0.86$, $P < 0.001$; *SI Appendix*, Fig. S6*A*) and springtails Collembola ($R = 0.68$, $P < 0.001$; *SI Appendix*, Fig. S6*B*) and geosmin concentrations. Recent work has revealed that various microbial species (28), especially Actinobacteria, produce geosmin and/or 2-methylisoborneol, which are volatile substances of terpenoids, to attract springtails and accomplish long-distance dispersal (17). In this way, microscopic arthropods feast upon these bacteria and serve as vectors for their dispersal through adherence to the springtails' surface and/or in springtail fecal pellets (29). Not surprisingly, our metagenomic analyses detect the genes coding for geosmin biosynthesis (such as *dxs*, *dxr*, *ispD*, *ispE*, *ispF*, *ispG*, *gcpE*, *ispH*, *IytB*, *idi*, *IDI*, *ZFPS*, and *cyc2*) in the Actinobacteria pivotal bin in our tomb samples with high relative abundances (Fig. 3*B* and Dataset S1). Moreover, we were able to quantify the concentrations of geosmin (2.90 to 16.1 ng/m^3) and 2-methylisoborneol (4.40 to 22.0 ng/m^3) in the air in the tomb (*SI Appendix*, Table S1). To provide further experimental evidence, we quantified the capacity of eight Pseudonocardiaceae strains (*SI Appendix*, Fig. S5) screened from this tomb to produce geosmin and found that these strains support high levels of geosmin production (0.80 to 6.00 ng/mL for geosmin and 8.60 to 429.67 ng/mL for 2-methylisoborneol) (*SI Appendix*, Table S2). To provide further evidence of Actinobacteria–Collembola associations, we conducted a microcosm interaction experiment and found that Actinobacteria (i.e., Pseudonocardiaceae) strains have a strong capacity to attract Collembola in closed controlled environments (Fig. 4 *A* and *B*). The videos (Movies S1 and S2) are vivid evidence to show how Collembola graze on Actinobacteria and help them to disperse by attaching to their bodies.

Together, all independent evidence substantiates interactions between Actinobacteria and springtails in this studied subterranean tomb. Since arthropods like low-stress environmental variables, such as stable hydrothermal conditions and fewer anthropogenic perturbations (*SI Appendix*, Figs. S6*B* and S7) (30), it is conceivable that Actinobacteria (and/or their spores) initially deterministically arrive in these tombs with the help of Collembola and/or stochastically arrive airborne (27). Subsequently, the release of geosmin from the tomb further attracts more Collembola outside, thus contributing to more Actinobacteria dispersal into the tomb. Such microbe–arthropod mutualism has been extensively recorded for mosquitoes and skin-associated bacteria (e.g., *Brevibacterium epidermidis* and *Corynebacterium minutissimum*) (31), amoebae and associated bacteria (e.g., Proteobacteria and Bacteroidetes) (32), and bark beetles and fungi (33). However, the influence of such interkingdom signaling mutualism between Actinobacteria and Collembola on the microbiomes colonizing historical cultural relics is virtually unknown. Our investigations provide evidence for such Actinobacteria–Collembola interactions, which could be

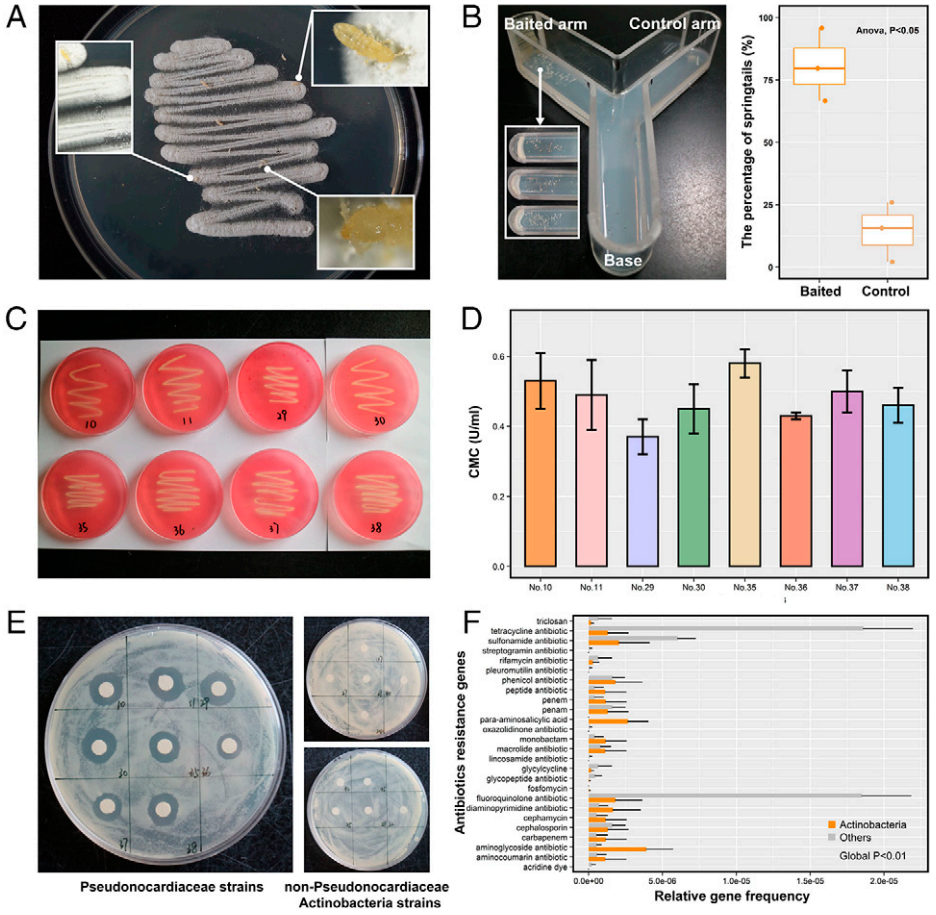

Fig. 4. Physiological assays and biological experiments of screened Pseudonocardiaceae strains. (*A*) Photographs of springtails *F. candida* feasting upon Pseudonocardiaceae strains and bringing them around on the CMC-Na agar medium. (*B*) The experiment of Actinobacteria–Collembola (Pseudonocardiaceae–*F. candida*) interaction over 30 h. The numbers of springtails *F. candida* baited with Pseudonocardiaceae were significantly higher than those of the unbaited control (80.73 vs. 14.54%, $P < 0.05$). (*C* and *D*) Hydrolytic zones of screened Pseudonocardiaceae strains on CMC-Na medium after 7 d (*C*) indicate their ability to degrade cellulose, which is further quantified by the DNS method (*D*). Error bars represent SD in (*D*). (*E* and *F*) The zones of inhibiting *B. subtilis* on LB medium using the Kirby–Bauer antimicrobial susceptibility test indicate the antimicrobial ability of screened Pseudonocardiaceae strains (*E*), which well aligns with high relative frequencies of antibiotic-resistance genes of non-Actinobacteria bacterial taxa (i.e., others) in our metagenomics (*F*).

an important mechanism helping to explain the dispersal of microorganisms (e.g., Actinobacteria in this study) into subterranean tombs and/or caves from surrounding environments.

Intrakingdom Competition Allows Actinobacteria to Colonize and Thrive in the Tomb. Our findings suggest that intrakingdom competition mechanisms, associated with the greater metabolic efficiency and the production of antibiotic substances, could contribute to explain the dominance of Actinobacteria on walls and/or murals in this subterranean tomb. Actinobacteria can produce and excrete a mixture of carbohydrate enzymes and thereby utilize a wide range of complex and recalcitrant organic polymers, such as polysaccharides and lignocellulose (19, 34); however, this remarkable ability that allows them to establish and thrive on cultural relics (10, 35) is still poorly described. The analysis of the genome of the pivotal Actinobacteria bin in our metagenomics suggests that these taxa hold a variety of carbohydrate-active enzyme (CAZyme) classes with high proportions, such as glycoside hydrolases (GHs), glycosyl transferases (GTs), the carbohydrate-binding modules (CBMs), carbohydrate esterases (CEs), auxiliary activities (AAs), and polysaccharide lyases (PLs) (Dataset S2). This observation is further supported by physiological assays of the growth of the screened Pseudonocardiaceae strains on carboxymethyl cellulose sodium (CMC-Na) agar medium and of their detected cellulase activities (Fig. 4 *C* and *D* and *SI Appendix*, Table S3). Carbon resources in items representing cultural heritage sites always occur as follows: 1) original constituents of works of art [e.g., base layers, the direct carrier of murals, are usually made of cellulose, wood, animal glue, and proteins from parchment, silk, and wool (36)]; 2) external residues [for example, subterranean dripping water in the tomb contains lignin and humic substances (10)]; and 3) polymer materials used for protection. The application of large-molecular-mass polymers (e.g., adhesives, consolidants, and protective coatings) was popular for cultural relic protection during the 1980s to 1990s (37). Murals were also coated by cellulose nitrate in the Dahuting Han Dynasty Tomb in the 1990s (*SI Appendix*, Fig. S9). These polymer organic substances can act as media or resources to stimulate Actinobacteria. Furthermore, abundances of CAZymes are found to be significantly higher in Actinobacteria compared with those in other bacteria (i.e., others) ($P < 0.01$) in our metagenomics (Fig. 3*C*). Also, cellulase activities of Pseudonocardiaceae strains are higher than those of non-Pseudonocardiaceae strains ($P < 0.05$; *SI Appendix*, Table S3). In this respect, Actinobacteria, Pseudonocardiaceae could have a metabolic advantage over other bacteria (namely, exploitative competition) in thriving in the Dahuting Han Dynasty Tomb.

In addition, interference competition could also help to explain the domination of Actinobacteria. Actinobacteria are well-known as producers of antimicrobial substances (20). Consistently, gene

clusters for the biosyntheses of several representative antimicrobial substances are found in the pivotal Actinobacteria bin (Fig. 3*D* and Dataset S3). In particular, the gene clusters coding for biosyntheses of antimicrobial substances present high similarity scores [e.g., showdomycin (38), promysalin (39), curacomycin (40), neopolyoxin C (41), and thienamycin (42)]. Physiological assays further support these observations, and find that the Pseudonocardiaceae strains exclusively have negative effects on the growth of gram-positive bacteria, such as *Bacillus subtilis* (Fig. 4*E*). This result is also in agreement with the larger proportions of antibiotic-resistance genes of non-Actinobacteria bacterial taxa (i.e., others) in our metagenomics (Fig. 4*F*). In contrast, 10 non-Pseudonocardiaceae strains screened have no inhibiting effects on *B. subtilis* (Fig. 4*E*). Thus, in principle, our analyses support that Actinobacteria, Pseudonocardiaceae could suppress competitors via interference competition (Fig. 3*A*).

Conclusion

In reality, we can never know comprehensively how microorganisms disperse and thrive in the tomb and there should be multiple mechanisms functioning alone and/or in combination. However, our evidence gives several possible mechanisms derived from sporadic evidence aligning with previous reports. In summary, our work reveals that multikingdom biological interactions (i.e., interkingdom mutualism and intrakingdom competition) drive the microbiome in the Dahuting Han Dynasty Tomb (Fig. 5). As one possible source, Actinobacteria disperse into the tomb with the help of Collembola via an interkingdom signaling mechanism. Once Actinobacteria arrive in the tomb, they start a machinery of enzymes that allows them to more readily thrive on relics than other bacteria (i.e., intrakingdom exploitative competition). Besides, intrakingdom interference competition could also help them to dominate the microbiome in the tomb via the production of antimicrobial substances that exclude bacterial competitors. Taken together, our work highlights the importance of understanding the ecology of the microbiomes thriving on historical cultural relics and remains in subterranean tombs and/or caves, to help preserve cultural heritages and ensure their long-term conservation for future generations.

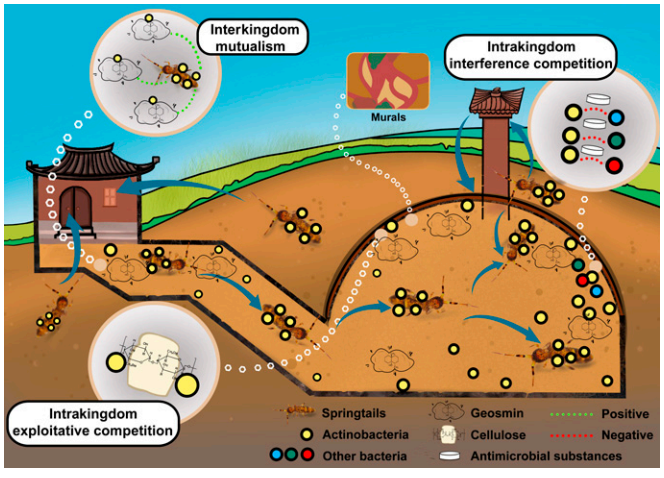

Fig. 5. Sketching map of multikingdom interactions governing the microbiome of the cultural relics in the Dahuting Han Dynasty Tomb. In brief, when the tomb is excavated and open to external environments, Actinobacteria are deterministically dispersed into the tomb from the surrounding environments with the help of Collembola and stochastically dispersed via air. Once inside, they start machineries of cellulases and antimicrobial substances, which allows them to readily colonize and thrive on tomb walls. Subsequently, their production of geosmin attracts more Collembola from outside environments, thereby increasing the dispersal of Actinobacteria into the tomb. Through this loop, Actinobacteria finally dominate the microbiome throughout the tomb.

Materials and Methods

Description of the Dahuting Han Dynasty Tomb. The Dahuting Han Dynasty Tomb (34°31′N, 113°18′E) is located in Xinmi City (Henan Province, China), which has a mean annual average temperature of 14.7 °C and mean annual precipitation of ∼663 mm. The tomb is 7.8 m below ground level and composed of four ear chambers as well as one corridor around an atrium (*SI Appendix*, Fig. S1*A*). The gas exchange between the tomb and surrounding environments occurs continuously via ventilation through corridor windows and a ventilation tower and through the connecting corridor (*SI Appendix*, Fig. S1*B*). The tomb walls were treated with nitrocellulose as a protective agent for conservation in the 1990s, which was deemed an effective protective practice in the 1980s to 1990s. A Fourier transform infrared (FT-IR) spectrometer (Nicolet iN10 MX FT-IR microscope; Thermo Scientific) indicated that the main chemical components of the surface of tomb walls were large-molecular-mass cellulose-like substances (*SI Appendix*, Fig. S9). Photomicrographs of white colonizers were taken using a JEOL JSM-6610LV scanning electron microscope (Japan).

Sampling of Microbial Communities in the Tomb and Surrounding Soils. A total of 10 samples on walls of the tomb and 12 soil samples from the area surrounding the tomb were collected (*SI Appendix*, Fig. S1). In detail, the samples on the walls in the Dahuting Han Dynasty Tomb presented macroscopic white colonizers. A sterile scalpel was carefully used to scrape these colonies to prevent damage to the mural and/or wall ontology. Upon collection, the samples were immediately delivered on ice, and frozen when arriving at the laboratory.

Assessing Temperature and Humidity Inside and Outside the Tomb. Due to long-term closure to visitors (nearly 30 y), the Dahuting Han Dynasty Tomb is characterized by complete darkness and relatively constant air humidity and temperature. This finding is corroborated by the higher constancy index of temperature and humidity variables measured in the tomb, compared with surrounding environments. The air temperature and humidity inside and outside the tomb were measured by electronic temperature and humidity recorders (HOBO; MX2301) and recorded every 10 min from 25 November 2020 to 25 April 2021 (*SI Appendix*, Fig. S7). Then, the stability of the air temperature and humidity of both the tomb and surrounding environments for 6 mo was estimated by the constancy index. The constancy index was defined as μ/σ, where μ was the mean value of the air temperature and humidity for a time period and σ was its SD over the same interval. A greater constancy index indicated a higher stability status.

Environmental DNA Extraction and Amplicon High-Throughput Sequencing of Fragments of Bacterial 16S rRNA Genes and Eukaryotic 18S rRNA Genes. Genomic DNA was extracted using a FastDNA SPIN Kit for soil (MP Biomedicals) with negative control of ddH_2O, following the manufacturer's instructions. The bacterial 16S rRNA gene V4 to V5 fragments were amplified using the primer pairs 519F (5′-CAGCMGCCGCGGTAATWC-3′) and 907R (5′-CCGTCAATTCMTTTRAGTTT-3′). Amplifications were carried out using the following thermal conditions: 94 °C for 5 min; 30 cycles of 94 °C for 30 s, 55 °C for 30 s, and 72 °C for 45 s; and a final extension at 72 °C for 10 min. The eukaryotic 18S rRNA gene V4 fragments were amplified using the primer pairs 528F (5′-GCGGTAATTCCAGCTCCAA-3′) and 706R (5′-AATCCRAGAATTTCACCTCCAA-3′). Amplifications were carried out using thermal conditions as follows: 98 °C for 30 s; 30 cycles of 98 °C for 10 s, 53 °C for 30 s, and 72 °C for 30 s; and a final extension at 72 °C for 10 min. The 5-bp barcoded oligonucleotides were fused to the forward primer to distinguish different samples. The PCR products for each sample were pooled and purified using the QIAquick PCR Purification Kit (QIAGEN) and quantified using a NanoDrop ND-2000 (Thermo Scientific). The preparation and processing of amplicon high-throughput sequencing libraries and data processing are fully described in Liu et al. (43). In total, 1,321,520 high-quality bacterial 16S rRNA and 457,457 high-quality eukaryotic 18S rRNA gene reads (after excluding fungi) were obtained for downstream ecological analyses. Taxonomy was assigned to bacterial and eukaryotic OTUs (at 97% similarity) with reference to the SILVA 138 database. In addition, the dominant

microbiome (both taxa composition and community differences) revealed by rarified OTU tables of both bacteria (29,066 reads per sample) and eukaryotes (1,108 reads per sample) was also analyzed in parallel (*SI Appendix*, Figs. S10–S12) and the same outcomes were obtained.

qPCR of 16S rRNA, 18S rRNA, and Internal Transcribed Spacer rRNA Genes. The copy numbers of bacterial 16S rRNA, fungal internal transcribed spacer (ITS) rRNA, and eukaryotic 18S rRNA gene fragments in each sample were quantified by real-time qPCR using the primers 519F/907R, ITS3/ITS4, and 82F/Euk516R, respectively. A detailed description of the qPCR procedure is provided by Feng et al. (44).

Microbial Phylotype Cooccurrence Network Analysis. Phylogenetic molecular ecological networks (pMENs) were constructed and evaluated using the random matrix theory–based network approach based on the amplicon reads (45). pMENs construction and analyses were performed using a pipeline written in Java and Perl scripts (http://ieg4.rccc.ou.edu/mena/) (46). Then, the constructed network graphs were visualized by Gephi software. More information about pipeline theories and properties can be found in Zhou et al. (47). In detail, all Pseudonocardiaceae and Collembola taxa were first conducted for the interkingdom cooccurrence network. The seven highest-abundance Collembola taxa showed significantly positive interactions with Pseudonocardiaceae OTU1 (*SI Appendix*, Fig. S8*A*). For the intrakingdom (bacterial) cooccurrence network, we found 217 bacterial taxa and 761 linkages. Herein, Pseudonocardiaceae OTU1 accounted for more than 50% of reads of 101 Pseudonocardiaceae taxa in all samples. There were significantly negative interactions between Pseudonocardiaceae OTU1 and 60 bacterial taxa (*SI Appendix*, Fig. S8*B*). Finally, we used the above-mentioned Pseudonocardiaceae OTU1 and 60 bacterial and 7 highest-abundance Collembola taxa to build the multikingdom cooccurrence network (Fig. 3*A*).

Shotgun Metagenomic Sequencing of Tomb Samples and Metagenomic Analyses for Physiological Features. Approximately 10 to 20 μg of DNA was retrieved from each of the 10 tomb samples for shotgun metagenomic sequencing. Sequencing libraries were prepared using the NEBNext Ultra DNA Library Prep Kit (New England Biolabs) following the manufacturer's protocols. Adapters were ligated to the blunt-end fragments. Metagenomic sequence data for the 10 tomb samples were produced using Illumina NovaSeq 6000 instruments at Guangdong Magigene Biotechnology Co. Ltd. In total, ∼10-Gbp paired-end Illumina data were obtained for each sample. Raw reads were trimmed to eliminate adapters and low-quality reads with Trimmomatic v0.36 (48). In brief, adapters were eliminated, reads with ≥5 "N" were removed, and low-quality reads were filtered. High-quality sequencing data from each sample were individually assembled into contigs using MEGAHIT v1.0.6 (–k-min 35 –k-max 95 –k-step 20). All reads not used in the single assembly were combined and then MEGAHIT software was used for mixed assemblies with the same parameters as the single assembly. The contigs (≥500 bp) assembled from both single and mixed contigs were all predicted to have open reading frames by MetaGeneMark v3.38. CD-HIT v4.7 was adopted to remove redundancy and obtain unigenes, which were clustered by identity at 95% and coverage at 90%, and the longest to the representative sequences was chosen. Gene coverage was calculated using BBMap v36.x with the parameters $k = 14$, minid = 0.97, and build = 1. Based on the number of mapped reads and the length of the gene, the abundance information of each gene in each sample was statistically analyzed. The relative abundance of a given gene functional category against the KEGG (Kyoto Encyclopedia of Genes and Genomes) database was calculated based on the gene coverage result using in-home Perl scripts (49). The SILVA 138 database was used for species identification by read mapping.

The high-quality reads of all 10 samples (∼100-Gbp paired-end Illumina data in total) were combined and assembled into contigs using MEGAHIT v1.0.6 (–k-min 35 –k-max 115 –k-step 20). These contigs were binned using MetaBAT with default parameters (50), and this process considered both tetranucleotide frequencies and scaffold coverage information. All bins generated were subjected to RefineM v0.0.14 and then to manual examination for further refinement (51). CheckM was used to assess the completeness and contamination of these genome bins through the identification and quantification of single-copy marker genes (52). The taxonomic identification of the bins with the top 50 highest abundances was conducted using reference genomes in the National Center for Biotechnology Information (NCBI) Nucleotide database. The bins affiliated with the Actinobacteria phylum were sorted. Herein, the top five bins (accounting for ∼60% of sequences of the total recognized bins) were merged into one pivotal bin (named the pivotal Actinobacteria bin afterward) with 7-Mbp size. The genome of this pivotal Actinobacteria bin was further analyzed for the geosmin metabolic pathway, sequences encoding cellulases, and gene clusters for the biosyntheses of antimicrobial substances.

The automated gene prediction of the sequences was conducted using an open-source gene prediction program called Prodigal (prokaryotic dynamic programming gene-finding algorithm) v2.6.3 (53), and the protein-coding genes were assigned to the NCBI nr database, eggNOG (evolutionary genealogy of genes: nonsupervised orthologous groups), and KEGG (https://www.kegg.jp/) databases for functional annotation with an *e*-value threshold of 10^{-5}. Ten enzymes were recognized to complete the geosmin biosynthesis and a database containing 10 homologous genes encoding each enzyme was generated. To identify genes related to geosmin biosynthesis (54), sequences were blasted with the above-mentioned database via NCBI Blast (basic local alignment search tool) (https://blast.ncbi.nlm.nih.gov/Blast.cgi) (55). A public database (eggNOG; http://eggnog.embl.de) (56) for orthology relationship, gene evolutionary history, and functional annotation was used for the identification of CAZymes, containing GHs, GTs, CEs, CBMs, PLs, AAs of Actinobacteria and other bacterial taxa. A percent identity >0.3 was chosen as a threshold for the above analysis. Gene clusters for the biosyntheses of secondary metabolics were mined by antiSMASH (https://antismash-db.secondarymetabo lites.org/) (57). Antimicrobial substances with similarity score >0.5 were kept in this study. Resistance gene identifier (RGI) software was used to identify antibiotic-resistance genes of Actinobacteria and other bacterial taxa with the Strict algorithm (defined as over 95% identity, regardless of alignment length; https://github.com/arpcard/rgi) based on the public database CARD (Comprehensive Antibiotic Research Database; https://card.mcmaster.ca/analyze/rgi).

Culturing Actinobacteria Strains. GAUZE's medium plus 0.01% potassium dichromate was used to screen Actinobacteria strains. Yeast malt extract medium (58) was used to culture Actinobacteria strains and to exhibit their differences in colony morphology. CMC-Na medium was used to ensure their cellulose-degrading abilities. Detailed information on each medium is below. GAUZE's agar medium (per liter): soluble starch 20.0 g, KNO_3 1 g, NaCl 0.5 g, $K_2HPO_4 \bullet 3H_2O$ 0.5 g, $MgSO_4 \bullet 7H_2O$ 0.5 g, $FeSO_4 \bullet 7H_2O$ 0.01 g, agar 20.0 g, pH 7.3; yeast malt extract medium (per liter): malt extract 10.0 g, yeast extract 4.0 g, dextrose 4.0 g, agar 20.0 g, pH 7.3. CMC-Na agar medium (per liter): CMC-Na 20 g, KH_2PO_4 2.5 g, NaH_2PO_4 2.5 g, yeast extract 0.5 g, peptone 2.0 g, agar 20.0 g, pH 7.3.

Phylogenetic Identification of Screened Strains. The genomes of 18 strains screened were extracted by an E.Z.N.A. Bacterial DNA Kit (Omega Bio-Tek). The primer set 27F/1492R was then used to amplify the ca. 1,500-bp fragment of the 16S rRNA gene fragment. PCR was carried out in 50-μL reaction mixtures with the following components: each deoxynucleoside triphosphate at a concentration of 1.25 mM; 2 μL (15 μM each) of forward and reverse primers; 2 U of Taq DNA polymerase (TaKaRa); and 50 ng of DNA. The PCR profile consisted of an initial denaturation at 95 °C for 5 min; 35 cycles of denaturation at 95 °C for 1 min, annealing at 58 °C for 90 s, and extension at 72 °C for 2 min; and a final extension at 72 °C for 10 min. Three independent PCR products for each strain were mixed, purified using the QIAquick PCR Purification Kit (QIAGEN), and sent for Sanger dideoxy sequencing.

Together with the top three BLAST hits of homologous gene sequences and the Actinobacteria ribosomal gene sequences from cultured strains in GenBank, the representative clone sequences were used to build a basic phylogenetic tree by the neighbor-joining method using MEGA (molecular evolutionary genetics analysis) software v4.0 (59). The tree topology was further evaluated by different methods including minimum evolution and maximum parsimony. The phylogenetic relationships of bacterial ribosomal gene sequences to the closest homolog in the GenBank database were then inferred.

Physiological Assays of Screened Pseudonocardiaceae Strains. Cellulose-degrading abilities of all screened Actinobacteria strains were visualized by CMC-Na agar medium plus a Congo red staining test (60). The cellulase activity was further determined using the 3,5-dinitrosalicylic acid (DNS) method (61). In

brief, the polysaccharide substrates tested were CMC. The assays of hydrolytic activity were performed at 60 °C for 30 min. One enzymatic unit of activity was defined as the amount of enzyme that released 1 μmol of reducing sugar equivalents per minute.

The Kirby–Bauer antimicrobial susceptibility test was conducted with paper disks permeated by culture supernatant of yeast malt medium for screened Actinobacteria strains atop a slab of Luria-Bertani (LB) agar culturing the strain of *B. subtilis* (62). High-resolution time-of-flight mass spectrometry combined with high-performance liquid chromatography was used for detection and determination of tetracycline and fluoroquinolone antibiotics in the culture supernatant of screened Pseudonocardiaceae strains. However, the known tetracycline and fluoroquinolone antibiotics were not detected in the database of Shimadzu Co. Ltd. In combination with inhibiting zones, there could be unknown antibiotics or other antimicrobial substances.

Measurement of Geosmin and 2-Methylisoborneol in the Air of the Tomb and in the Headspace of Screened Pseudonocardiaceae Strain Cultures. The volatile organic compounds geosmin and 2-methylisoborneol in the air of the tomb and of the headspace of 18 screened Actinobacteria strain cultures were respectively measured by Nanjing Liankai Environmental Testing Technology Co. Ltd., following the protocol of Becher et al. (17). In brief, 72 L of air was respectively collected in the atrium, corridor, and two chambers (*SI Appendix*, Fig. S1*A*) for 4 h by an air sampler (MH1200; Minhope). Methylene chloride was used as the absorption liquid. The air in the headspace of screened Pseudonocardiaceae strain cultures (for 5 d with yeast malt extract medium) was collected and absorbed in methylene chloride. Volatiles in the absorption liquid were analyzed by a coupled gas chromatograph–mass spectrometer (GC-MS) (6890 GC and 5975 MS; Agilent Technologies) operated in electron impact ionization mode at 70 eV. The GC was equipped with an HP-5MS (Agilent Technologies) fused silica capillary column (60 m × 0.25 mm^2; $d_f = 0.25$ μm). Helium was used as the carrier gas at an average linear flow rate of 35 $cm \cdot s^{-1}$.

Pseudonocardiaceae–Collembola Interaction Experiment. Springtails were tested for attraction to the Pseudonocardiaceae strain and/or geosmin in a device with three chambers linked by Y-shaped glass tubing (Fig. 4*B*), following the design of an olfactometer (63). The Y-shaped tubing (30-mm inner diameter) had one 120-mm-long base and two 120-mm-long arms. Before the experiment, springtails *Folsomia candida* were starved for 24 h. Springtails *F. candida* ($n = 50$) were placed at the end of the base. Seven-day Pseudonocardiaceae strain colonies were placed at one side arm as an odor-release compartment; the other side arm acted as the control compartment. The difference in the number of springtails was then evaluated between the odor-release and control compartments. The experiment was performed for 30 h at 25 °C and 60 ± 5% relative humidity and in the dark. There were triplicates.

Statistical Analysis. A Venn diagram analysis was used to compare bacterial and eukaryotic OTUs existing in more than 8/10 samples between the tomb and surrounding soils, using the R package VennDiagram (v1.6.20) (64). The environmental factors shifting bacterial and eukaryotic community compositions as well as their dominant species between the tomb and surrounding soils were revealed by RDA, based on the Jaccard distance, using the R VEGAN package (65). Their significant differences were further visualized by Bray–Curtis distance–based heatmaps and evaluated by permutational multivariate ANOVA tests (66). Differences of relative frequencies of CAZyme-encoding genes measured by G_k values between Actinobacteria and other bacterial taxa, the difference in cellulase activities between Pseudonocardiaceae and non-Pseudonocardiaceae strains, as well as the difference in number of springtails between the odor-release and control compartments were respectively evaluated with an independent-samples *t* test followed by Levene's tests using IBM Statistical Product and Service Solutions (SPSS) Statistics for Windows (v13). Differences in relative frequencies of antibiotic-resistance genes among non-Actinobacteria bacterial taxa (i.e., others) were evaluated with one-way ANOVA followed by post hoc Tukey's honestly significant difference tests. $P < 0.05$ and $P < 0.01$ were considered significantly and highly significantly different, respectively.

Data Availability. The amplicon sequences, shotgun metagenomics, and screened Actinobacteria strain sequences reported in this article have been deposited in the NCBI BioProject and GenBank databases (accession nos. PRJNA721777, PRJNA745276, and OL444665 to OL444682, respectively). All other study data are included in the article and/or supporting information.

ACKNOWLEDGMENTS. This work was supported by the National Key R&D Program (2019YFC1520700), the National Natural Science Foundation of China (42177297), Chinese Academy of Sciences (CAS) Strategic Priority Research Program Grant XDA28010302, and the Youth Innovation Promotion Association, CAS (Member No. 2014271). M.D.-B. is supported by a Ramón y Cajal Grant (RYC2018-025483-I), a project from the Spanish Ministry of Science and Innovation (PID2020-115813RA-I00), and Project Plan Andaluz de Investigación, Desarrollo e Innovación 2020 from the Junta de Andalucía (P20_00879).

Author affiliations: [a]State Key Laboratory of Soil and Sustainable Agriculture, Institute of Soil Science, Chinese Academy of Sciences, Nanjing 210008, China; [b]University of Chinese Academy of Sciences, Beijing 100049, China; [c]College of Chemical Engineering, Nanjing Forestry University, Nanjing 210037, China; [d]Guangdong Magigene Biotechnology Co. Ltd., Shenzhen 510300, China; [e]School of Architecture, Southeast University, Nanjing 210096, China; [f]Key Laboratory of Urban and Architectural Heritage Conservation of the Ministry of Education, Southeast University, Nanjing 210096, China; [g]College of Biotechnology and Pharmaceutical Engineering, Nanjing Tech University, Nanjing 211816, China; [h]Soil Ecology Lab, College of Resources and Environmental Sciences, Nanjing Agricultural University, Nanjing 210095, China; [i]The Conservation Institute, Dunhuang Academy, Dunhuang 736200, China; [j]Instituto de Recursos Naturales y Agrobiología de Sevilla, Consejo Superior de Investigaciones Científicas (CSIC), Sevilla E-41012, Spain; and [k]Unidad Asociada CSIC-UPO (BioFun), Universidad Pablo de Olavide (UPO), Sevilla 41013, Spain

1. F. Castellani, Historical monuments: The film crew. *Nature* **433**, 100–101 (2005).
2. X. B. Liu, R. J. Koestler, T. Warscheid, Y. Katayama, J. D. Gu, Microbial deterioration and sustainable conservation of stone monuments and buildings. *Nat. Sustain.* **3**, 991–1004 (2020).
3. C. Holden, Cave paintings in jeopardy. *Science* **297**, 47 (2002).
4. F. Bastian, V. Jurado, A. Nováková, C. Alabouvette, C. Saiz-Jimenez, The microbiology of Lascaux Cave. *Microbiology (Reading)* **156**, 644–652 (2010).
5. F. Stomeo, M. C. Portillo, J. M. Gonzalez, L. Laiz, C. Saiz-Jimenez, Pseudonocardia in white colonizations in two caves with Paleolithic paintings. *Int. Biodeterior. Biodegradation* **62**, 483–486 (2008).
6. S. Cuezva, S. Sanchez-Moral, C. Saiz-Jimenez, J. C. Canaveras, Microbial communities and associated mineral fabrics in Altamira Cave, Spain. *Int. J. Speleol.* **38**, 83–92 (2009).
7. F. Bastian, C. Alabouvette, Lights and shadows on the conservation of a rock art cave: The case of Lascaux Cave. *Int. J. Speleol.* **38**, 55–60 (2009).
8. L. Allemand, P. G. Bahn, Best way to protect rock art is to leave it alone. *Nature* **433**, 800 (2005).
9. M. C. Portillo, C. Saiz-Jimenez, J. M. Gonzalez, Molecular characterization of total and metabolically active bacterial communities of "white colonizations" in the Altamira Cave, Spain. *Res. Microbiol.* **160**, 41–47 (2009).
10. M. Diaz-Herraiz *et al.*, The actinobacterial colonization of Etruscan paintings. *Sci. Rep.* **3**, 1440 (2013).
11. L. Alonso *et al.*, Anthropization level of Lascaux Cave microbiome shown by regional-scale comparisons of pristine and anthropized caves. *Mol. Ecol.* **28**, 3383–3394 (2019).
12. C. J. McNamara, R. Mitchell, Microbial deterioration of historic stone. *Front. Ecol. Environ.* **3**, 445–451 (2005).
13. H. Abdulla, E. May, M. Bahgat, A. Dewedar, Characterisation of Actinomycetes isolated from ancient stone and their potential for deterioration. *Pol. J. Microbiol.* **57**, 213–220 (2008).
14. K. Sterflinger, G. Piñar, Microbial deterioration of cultural heritage and works of art–Tilting at windmills? *Appl. Microbiol. Biotechnol.* **97**, 9637–9646 (2013).
15. A. K. Shaw, N. Narayanan, D. E. Stanton, Let's move out together: A framework for the intersections between movement and mutualism. *Ecology* **102**, e03419 (2021).
16. L. K. Ho *et al.*, Chemical entrapment and killing of insects by bacteria. *Nat. Commun.* **11**, 4608 (2020).
17. P. G. Becher *et al.*, Developmentally regulated volatiles geosmin and 2-methylisoborneol attract a soil arthropod to *Streptomyces* bacteria promoting spore dispersal. *Nat. Microbiol.* **5**, 821–829 (2020).
18. D. M. Cornforth, K. R. Foster, Competition sensing: The social side of bacterial stress responses. *Nat. Rev. Microbiol.* **11**, 285–293 (2013).
19. F. M. Medie, G. J. Davies, M. Drancourt, B. Henrissat, Genome analyses highlight the different biological roles of cellulases. *Nat. Rev. Microbiol.* **10**, 227–234 (2012).
20. D. A. van Bergeijk, B. R. Terlouw, M. H. Medema, G. P. van Wezel, Ecology and genomics of Actinobacteria: New concepts for natural product discovery. *Nat. Rev. Microbiol.* **18**, 546–558 (2020).
21. C. Saiz-Jimenez *et al.*, Conservation. Paleolithic art in peril: Policy and science collide at Altamira Cave. *Science* **334**, 42–43 (2011).
22. E. Baquero, R. Jordana, L. Labrada, C. G. Luque, A new species of *Pseudosinella* Schäffer, 1897 (Collembola, Entomobryidae) from Altamira Caves (Cantabria, Spain). *ZooKeys* **989**, 39–54 (2020).
23. S. Jantarit, K. Surakhamhaeng, L. Deharveng, The multiformity of antennal chaetae in *Troglopedetes* Joseph, 1872 (Collembola, Paronellidae, Troglopedetinae), with descriptions of two new species from Thailand. *ZooKeys* **987**, 1–40 (2020).
24. J. G. Palacios-Vargas, Acheroxenylla (Collembola, Hypogastruridae), first record from the Americas with description of a new species from a Peruvian cave. *Subterr. Biol.* **34**, 109–119 (2020).
25. Z. Huang, F. Zhao, Y. Li, J. Zhang, Y. Feng, Variations in the bacterial community compositions at different sites in the tomb of Emperor Yang of the Sui Dynasty. *Microbiol. Res.* **196**, 26–33 (2017).

26. M. Vellend, Conceptual synthesis in community ecology. *Q. Rev. Biol.* **85**, 183–206 (2010).
27. M. Saarela *et al.*, Heterotrophic microorganisms in air and biofilm samples from Roman catacombs, with special emphasis on actinobacteria and fungi. *Int. Biodeterior. Biodegradation* **54**, 27–37 (2004).
28. Y. Yamada *et al.*, Terpene synthases are widely distributed in bacteria. *Proc. Natl. Acad. Sci. U.S.A.* **112**, 857–862 (2015).
29. M. Rohlfs, *Streptomyces*' scent attracts spore dispersers. *Nat. Microbiol.* **5**, 780–781 (2020).
30. J. H. Carpenter, Forty-year natural history study of *Bahalana geracei* Carpenter, 1981, an anchialine cave-dwelling isopod (Crustacea, Isopoda, Cirolanidae) from San Salvador Island, Bahamas: Reproduction, growth, longevity, and population structure. *Subterr. Biol.* **37**, 105–156 (2021).
31. N. O. Verhulst *et al.*, Differential attraction of malaria mosquitoes to volatile blends produced by human skin bacteria. *PLoS One* **5**, e15829 (2010).
32. E. Sallinger, M. S. Robeson, T. S. Haselkorn, Characterization of the bacterial microbiomes of social amoebae and exploration of the roles of host and environment on microbiome composition. *Environ. Microbiol.* **23**, 126–142 (2021).
33. F. Zhou *et al.*, Bacterial volatile ammonia regulates the consumption sequence of D-pinitol and D-glucose in a fungus associated with an invasive bark beetle. *ISME J.* **11**, 2809–2820 (2017).
34. Y. Bao *et al.*, Important ecophysiological roles of non-dominant Actinobacteria in plant residue decomposition, especially in less fertile soils. *Microbiome* **9**, 84 (2021).
35. J. L. Gonzalez-Pimentel *et al.*, Yellow coloured mats from lava tubes of La Palma (Canary Islands, Spain) are dominated by metabolically active Actinobacteria. *Sci. Rep.* **8**, 1944 (2018).
36. O. Ciferri, Microbial degradation of paintings. *Appl. Environ. Microbiol.* **65**, 879–885 (1999).
37. F. Cappitelli, E. Zanardini, C. Sorlini, The biodeterioration of synthetic resins used in conservation. *Macromol. Biosci.* **4**, 399–406 (2004).
38. H. Nishimura *et al.*, Showdomycin, a new antibiotic from a *Streptomyces* sp. *J. Antibiot.* **17**, 148–155 (1964).
39. W. Li *et al.*, Promysalin, a salicylate-containing *Pseudomonas putida* antibiotic, promotes surface colonization and selectively targets other *Pseudomonas*. *Chem. Biol.* **18**, 1320–1330 (2011).
40. I. Kaweewan, H. Komaki, H. Hemmi, S. Kodani, Isolation and structure determination of new antibacterial peptide curacomycin based on genome mining. *Asian J. Org. Chem.* **6**, 1838–1844 (2017).
41. K. Kobinata *et al.*, Neopolyoxin-A, neopolyoxin-B, and neopolyoxin-C, new chitin synthetase inhibitors. *Agric. Biol. Chem.* **44**, 1709–1711 (1980).
42. J. R. Moran-Diaz *et al.*, Correlation study of antibacterial activity and spectrum of penicillins through a structure-activity relationship analysis. *Med. Chem. Res.* **28**, 1529–1546 (2019).
43. W. Liu *et al.*, Balanced stochastic versus deterministic assembly processes benefit diverse yet uneven ecosystem functions in representative agroecosystems. *Environ. Microbiol.* **23**, 391–404 (2021).
44. Y. Z. Feng, X. G. Lin, Z. J. Jia, J. G. Zhu, Identification of formate-metabolizing bacteria in paddy soil by DNA-based stable isotope probing. *Soil Sci. Soc. Am. J.* **76**, 121–129 (2012).
45. F. Luo *et al.*, Constructing gene co-expression networks and predicting functions of unknown genes by random matrix theory. *BMC Bioinformatics* **8**, 299 (2007).
46. Y. Deng *et al.*, Molecular ecological network analyses. *BMC Bioinformatics* **13**, 113 (2012).
47. J. Zhou *et al.*, Functional molecular ecological networks. *mBio* **1**, e00169-10 (2010).
48. A. M. Bolger, M. Lohse, B. Usadel, Trimmomatic: A flexible trimmer for Illumina sequence data. *Bioinformatics* **30**, 2114–2120 (2014).
49. Z. S. Hua *et al.*, Ecological roles of dominant and rare prokaryotes in acid mine drainage revealed by metagenomics and metatranscriptomics. *ISME J.* **9**, 1280–1294 (2015).
50. D. D. Kang, J. Froula, R. Egan, Z. Wang, MetaBAT, an efficient tool for accurately reconstructing single genomes from complex microbial communities. *PeerJ* **3**, e1165 (2015).
51. D. H. Parks *et al.*, Recovery of nearly 8,000 metagenome-assembled genomes substantially expands the tree of life. *Nat. Microbiol.* **2**, 1533–1542 (2017).
52. D. H. Parks, M. Imelfort, C. T. Skennerton, P. Hugenholtz, G. W. Tyson, CheckM: Assessing the quality of microbial genomes recovered from isolates, single cells, and metagenomes. *Genome Res.* **25**, 1043–1055 (2015).
53. D. Hyatt *et al.*, Prodigal: Prokaryotic gene recognition and translation initiation site identification. *BMC Bioinformatics* **11**, 119 (2010).
54. J. S. Dickschat, H. B. Bode, T. Mahmud, R. Müller, S. Schulz, A novel type of geosmin biosynthesis in myxobacteria. *J. Org. Chem.* **70**, 5174–5182 (2005).
55. C. Camacho *et al.*, BLAST+: Architecture and applications. *BMC Bioinformatics* **10**, 421 (2009).
56. J. Huerta-Cepas *et al.*, eggNOG 5.0: A hierarchical, functionally and phylogenetically annotated orthology resource based on 5090 organisms and 2502 viruses. *Nucleic Acids Res.* **47**, D309–D314 (2019).
57. K. Blin *et al.*, The antiSMASH database version 2: A comprehensive resource on secondary metabolite biosynthetic gene clusters. *Nucleic Acids Res.* **47**, D625–D630 (2019).
58. W. Xiang *et al.*, *Actinoalloteichus nanshanensis* sp. nov., isolated from the rhizosphere of a fig tree (*Ficus religiosa*). *Int. J. Syst. Evol. Microbiol.* **61**, 1165–1169 (2011).
59. K. Tamura, J. Dudley, M. Nei, S. Kumar, MEGA4: Molecular evolutionary genetics analysis (MEGA) software version 4.0. *Mol. Biol. Evol.* **24**, 1596–1599 (2007).
60. H. Puchtler, F. Sweat, Congo red as a stain for fluorescence microscopy of amyloid. *J. Histochem. Cytochem.* **13**, 693–694 (1965).
61. K. Lv *et al.*, Enhancing the catalytic activity of a GH5 processive endoglucanase from *Bacillus subtilis* BS-5 by site-directed mutagenesis. *Int. J. Biol. Macromol.* **168**, 442–452 (2021).
62. A. Wanger, "Disk diffusion test and gradient methodologies" in *Antimicrobial Susceptibility Testing Protocols*, R. Schwalbe, L. Steele-Moore, A. C. Goodwin, Eds. (CRC Press, 2007), pp. 53–73.
63. G. Bengtsson, K. Hedlund, S. Rundgren, Selective odor perception in the soil Collembola *Onychiurus armatus*. *J. Chem. Ecol.* **17**, 2113–2125 (1991).
64. H. Chen, P. C. Boutros, VennDiagram: A package for the generation of highly-customizable Venn and Euler diagrams in R. *BMC Bioinformatics* **12**, 35 (2011).
65. P. Dixon, VEGAN, a package of R functions for community ecology. *J. Veg. Sci.* **14**, 927–930 (2003).
66. M. J. Anderson, A new method for non-parametric multivariate analysis of variance. *Austral Ecol.* **26**, 32–46 (2001).